VIP *The following Communications have been judged by at least two referees to be "very important papers" and will be published online at www.angewandte.org soon:*

Books

News

Highlights

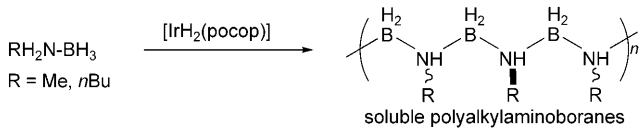

Soluble B–N Polymers

Taking the high road is what reactions of primary amine boranes do, according to results recently obtained by Manners and co-workers, when a homogeneous catalyst is used to prepare soluble aminoborane polymers and copolymers (see scheme; pocop = κ^3-1,3-$(OP^tBu_2)_2C_6H_3$). Such metal-catalyzed dehydrocoupling reactions for the synthesis of new B–N analogues of α-olefins are of fundamental interest for materials science.

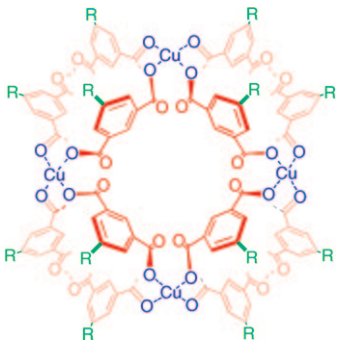

Supramolecular Chemistry

Space—the final frontier: Recent progress with metal–organic scaffolds (see picture for an example) to create synthetic ion channels and pores is summarized in this Highlight. The great advantage of this approach is access to a stable and large confined space from small structural units. Current breakthroughs promise future progress toward the synthesis of tubular structures and their multiple functionalization.

Contents

Minireviews

The chemical fingerprint of amber may be detected in terms of molecular components by pyrolysis GC–MS or in terms of ^{13}C NMR resonances. Understanding the components of amber can permit association with geographical and botanical sources. The picture shows an exudate with entrapped ants from a pine tree in the U.S. National Arboretum, Washington, DC. (Photograph by Chip Clark, National Museum of Natural History, Washington, DC).

Reviews

Putting the protein on the chip: This Review discusses chemical strategies, both covalent and noncovalent, for attaching proteins to surfaces to make protein biochips. Particular emphasis is put on the chemical specificity of protein attachment and on retention of protein function. Strategies for creating protein patterns (as opposed to protein arrays) are also presented.

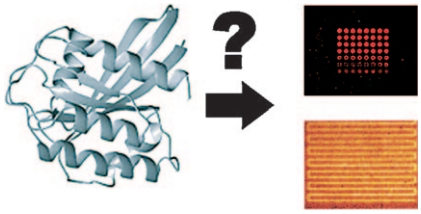

Communications

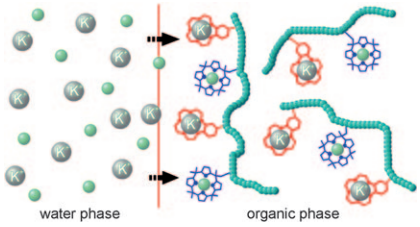

Fishing for KF: Potassium fluoride and chloride salts can be extracted from aqueous media using poly(methyl methacrylate)s containing pendant calix[4]pyrrole and crown ether groups (see picture). These polymers are able to extract these salts much more efficiently than calixpyrrole, crown ether, linked crown ether calixpyrrole monomers, polymers containing either recognition unit, or poly(methyl methacrylate) controls.

For the USA and Canada: ANGEWANDTE CHEMIE International Edition (ISSN 1433-7851) is published weekly by Wiley-VCH, PO Box 191161, 69451 Weinheim, Germany. Air freight and mailing in the USA by Publications Expediting Inc., 200 Meacham Ave., Elmont, NY 11003. Periodicals postage paid at Jamaica, NY 11431. US POSTMASTER: send address changes to *Angewandte Chemie*, Wiley-VCH, 111 River Street, Hoboken, NJ 07030. Annual subscription price for institutions: US$ 7225/6568 (valid for print and electronic / print or electronic delivery); for individuals who are personal members of a national chemical society prices are available on request. Postage and handling charges included. All prices are subject to local VAT/sales tax.

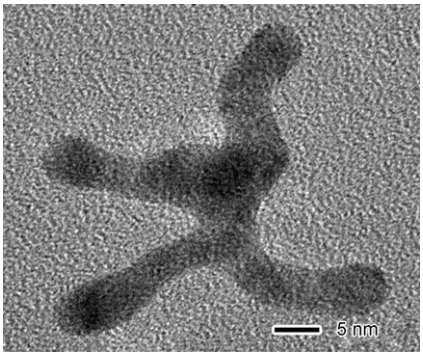

Self-destruct mechanism: Gold multipods are formed by a galvanic replacement reaction of AuCl with a self-destructive template consisting of a three-dimensional aggregate of magnetic iron nanoparticles. As a unique feature of this system, the template spontaneously falls apart during the reaction to automatically release the resultant gold multipods.

Gold Nanostructures

Switching Aromaticity: Conformations of [32]heptaphyrins(1.1.1.1.1.1.1) are dependent upon meso-aryl substituents, solvents, temperature, and protonation. Particularly, protonation of meso-pentafluorophenyl-substituted [32]heptaphyrin triggers conformational changes to form twisted aromatic Möbius structures (see picture), even at room temperature.

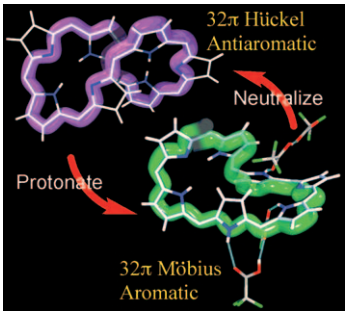

Aromaticity

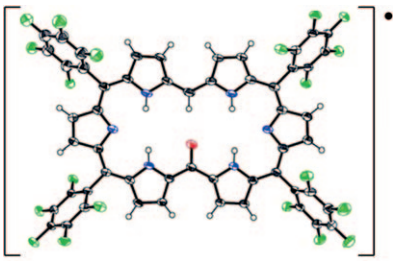

1

A stable radical: The title compound **1** has been synthesized as the first example of a meso-free variant and characterized as a strongly aromatic macrocycle with a spectacles-like planar conformation. The incorporation of free meso positions is promising for the exploration of novel structural and electronic properties.

Porphyrinoids

The observable histidine radical cation generated by collision-induced dissociation of the $[Cu^{II}(2,2':6',2''\text{-terpyridine})\text{-}(His)]^{+2}$ complex carries the positive charge on the protonated imidazole ring and the radical formally on the α carbon. This structure has been confirmed by infrared multiple photon dissociation (IRMPD) spectroscopy and density functional calculations.

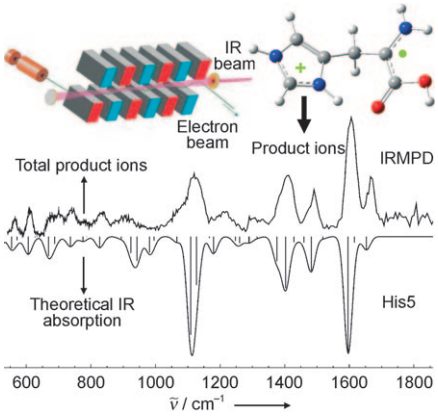

Radical Cations

Incredibly selective

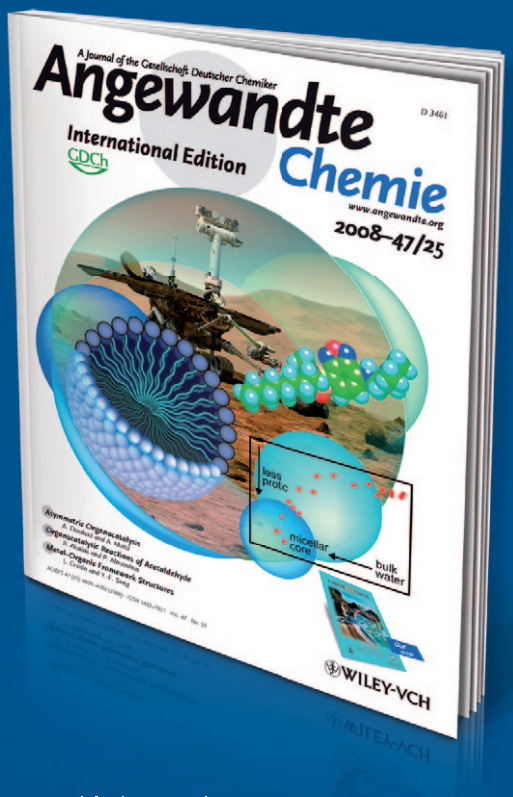

...!

Angewandte Chemie chooses its articles carefully. Most of its Reviews, Highlights, and Essays are written upon invitation, from authors who are among the very best in their fields. **Just 27 % of all submitted Communications in 2007 were accepted after peer review -** only about 1500 from nearly 5500. Communications that are judged to be exceptionally important within a particular field are featured as Very Important Papers **(VIPs)**.

GDCh
Gesellschaft Deutscher Chemiker

www.angewandte.org
service@wiley-vch.de

WILEY-VCH

A shift in focus: Fully oxidized pterins coordinated to ruthenium(II) undergo a first protonation at the nitrogen atom at the 1-position of the pyrimidinone moiety. Subsequent one-electron reduction induces an unprecedented proton shift from the nitrogen atom at the 1-position to that at the 8-position of the pyrazine moiety (see picture; C white, H yellow, N blue, O red).

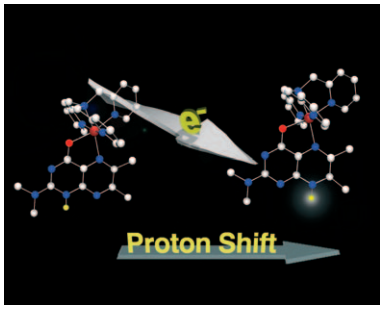

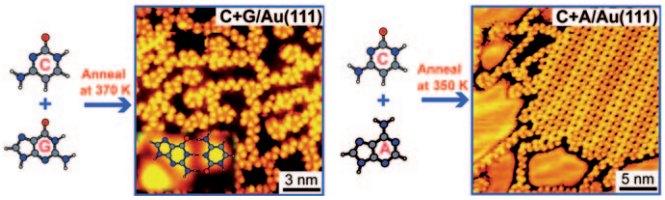

Surface Watson–Crick base pairing makes binary mixtures of the complementary nucleobases guanine (G) and cytosine (C) on Au(111) thermally stable up to the desorption temperature of the bases, whereas binary mixtures of the noncomplementary adenine (A) and cytosine segregate on heating (see STM images with DFT structures).

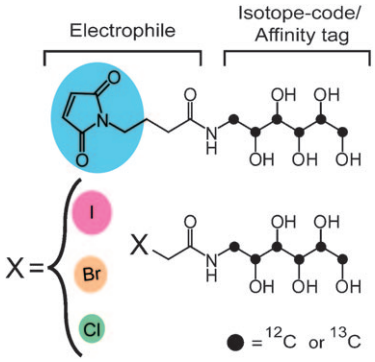

Another foot forward: Isotope-coded affinity tag (ICAT) reagents are versatile probes for footprinting dynamic protein structure. To render ICAT footprinting effective, a series of ICAT reagents with alkylation rates that span five orders of magnitude was designed. With this toolkit, an unprecedented range of Cys residues can be footprinted, including those deeply buried in the protein core and those involved in protein–protein interactions of modest affinity.

Sugared donuts: Reactions of hydrated chromium fluoride with *N*-ethyl-D-glucamine (H_5Etglu) in pivalic acid, in the presence of nickel carbonate, leads to heterometallic "glu-ed" rings. These rings allow for construction of polyring arrays, for example an assembly where four glued rings are attached to tetrapyridylporphyrin (see structure; F yellow, O red, N blue, Cr purple, Ni green, C black).

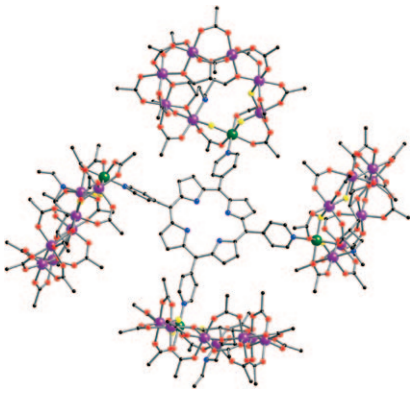

Contents

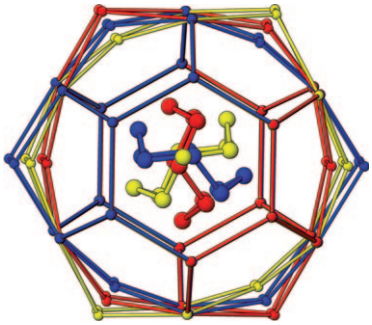

Cold guests lower the tone: The thermally induced phase transition in the hexagonal clathrate hydrate containing cyclooctane is reversible. This transition is most likely related to the freezing-in of the motion of the low-symmetry cyclooctane guest (see picture: colors indicate different orientations of the guest and associated distortions of the host).

Clathrate Structures

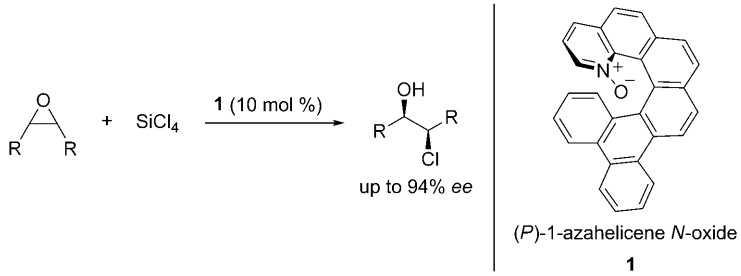

Asymmetric Catalysis

Helical Chiral Catalysts: The gram-scale synthesis of 1-azahelicenes, structural characterization of the corresponding *N*-oxides, and the application of this new family of catalysts to the catalytic, enantioselective ring-opening of *meso* epoxides is described (see scheme). Included is the first demonstration that the appropriate structural modifications beneath the plane of the pyridine *N*-oxide can serve as a powerful means for tuning the catalyst enantioselectivity.

Sturdy spinel: A mesoporous Li–Mn–O spinel ($Li_{1.12}Mn_{1.88}O_4$) with superior rate capability at ambient temperature is synthesized. Comparable stability to the bulk material at elevated temperatures is also observed, despite a surface area of 90 $m^2 g^{-1}$ for the mesopore, suggesting that the internal mesopore surfaces are more stable than the external surface.

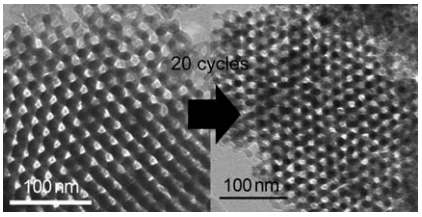

Mesoporous Cathodes

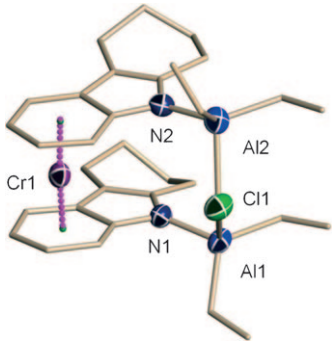

One more trimer: A series of chromium complexes of different oxidation states are employed as catalysts for the polymerization/oligomerization of ethylene. The results suggest a link between chromium oxidation state and catalytic performance, with Cr^{III} leading to oligomerization, Cr^{II} to polymerization, and Cr^{I} to selective trimerization.

Catalyst Design

Contents

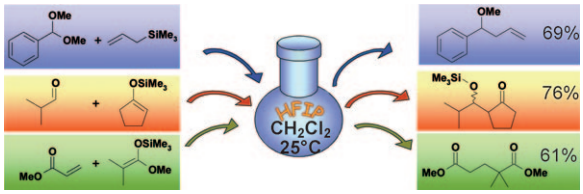

A credit to donation: A diverse range of electrophilic addition reactions, conventionally carried out using Lewis acid catalysts, have been performed in electrophilic media without acidic reagents. 1,1,1,3,3,3-Hexafluoro-2-propanol (HFIP) acts as an efficient hydrogen-bond donor and highly polar solvent for a wide range of substrates in reactions with Si-capped π donors.

Electrophilic Reaction Media

Two for one: Thermal generation of acylketenes in diol-containing substrates results in the title transformation. This transformation expands the scope of acylketene macrolactonizations and their application to the synthesis of complex macrolides. Triol and tetraol substrates have also been cyclized in highly regioselective fashion. Additionally, the challenging macrolactonization of a tertiary alcohol was achieved.

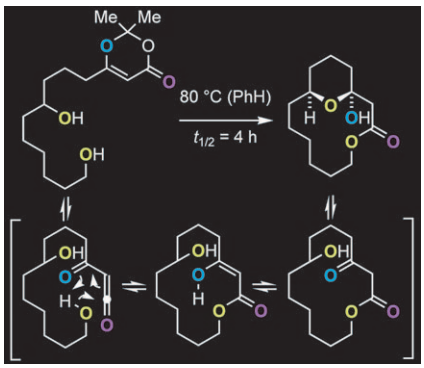

Synthetic Methods

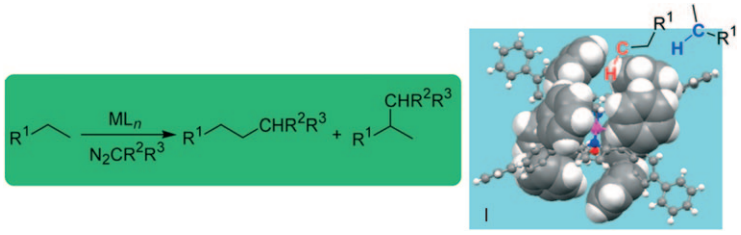

Primary C–H bond activation! A Rh complex of bis-pocket porphyrin **I** catalyzes carbenoid insertion into the C–H bonds of *n*-alkanes with a primary/secondary selectivity (per C–H bond) of up to 11.4:1 (see picture). Enantioselective secondary C–H bond functionalization catalyzed by a Rh complex of Halterman's chiral porphyrin features up to 93% *ee*. These reactions exhibit up to 6477 turnovers after the catalyst was recycled five times.

C–H Activation

A robust viral sensor was developed by bridging a pair of gold electrodes with antibody-coated peptide nanotubes. The nanotubes concentrated the target virus on their surface by molecular recognition between the antibody and the virus (see picture). The nanotubes fit perfectly within the electric field line distribution to enable the extremely sensitive impedimetric detection of viral particles.

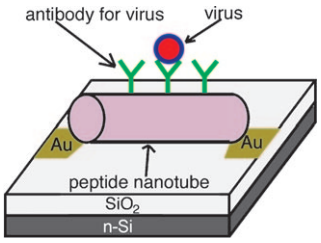

Bionanotechnology

Contents

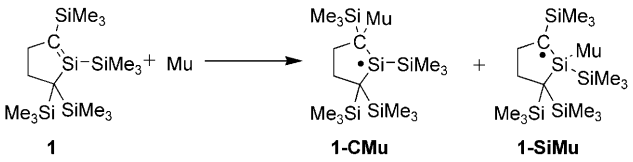

Taking the silenic route: Addition of a hydrogen atom analogue, muonium (Mu), to stable silene **1** gives rise to two distinct radical species, **1-CMu** and **1-SiMu**, allowing the relative reactivity of silenic carbon and silicon atoms to be probed. The former is the first reported example of a muoniated silyl radical. The radical species are detected by muon spin rotation and resonance spectroscopy (μSR).

Relative Reactivity

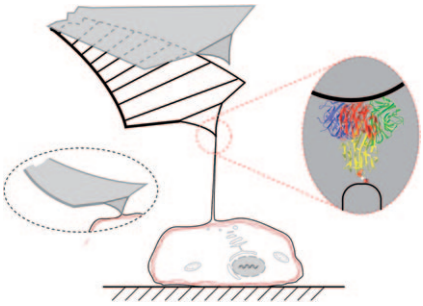

The name's Bond: Separated cells form membranous nanotubes whose tips are tethered by adhesive bonds (see picture). The lifetime of receptor–ligand interactions can be measured by using membrane nanotubes of living cells as constant force actuators. Because the nanotubes are extruded from living cells at conditions approaching the physiological, cellular processes can be both studied and utilized.

Cellular Adhesion

Supporting information is available on www.angewandte.org (see article for access details).

A video clip is available as Supporting Information on www.angewandte.org (see article for access details).

Service

Corrigenda

Covalently Linked Dimers of Clusters: Loop- and Dumbbell-Shaped Mn_{24} and Mn_{26} Single-Molecule Magnets

T. C. Stamatatos, K. A. Abboud, W. Wernsdorfer, G. Christou* 6694–6698

Angew. Chem. Int. Ed. **2008**, *47*

DOI 10.1002/anie.200801393

In this communication, the sentence starting 13 lines from the bottom of page 6696, left column, should read: "Extrapolating the plot above 4 K down to 0 K gives a value of about 52 $cm^3 K mol^{-1}$, suggesting an $S \approx 10$ ground state."

An Epilogue on the C_{78}-Fullerene Family: The Discovery and Characterization of an Elusive Isomer

K. S. Simeonov, K. Y. Amsharov, E. Krokos, M. Jansen* 6283–6285

Angew. Chem. Int. Ed. **2008**, *47*

DOI 10.1002/anie.200801922

In this communication, the identity of the fullerene isomer was incorrectly given. As investigated, $C_{78}Cl_{18}$ displays the connectivity pattern of $C_{78}(5)$, instead of $C_{78}(4)$ as stated.

